Axial U(1) symmetry near the pseudocritical temperature in $N_f = 2+1$ lattice QCD with chiral fermions

Sinya Aoki[a,b], Yasumichi Aoki[c], Hidenori Fukaya[d], Shoji Hashimoto[e,f], Issaku Kanamori[c], Takashi Kaneko[e,f,g], Yoshifumi Nakamura[c], Christian Rohrhofer[d], Kei Suzuki[h], and David Ward[d] (JLQCD Collaboration)

[a]*Center for Gravitational Physics, Yukawa Institute for Theoretical Physics, Kyoto 606-8502, Japan*

[b]*RIKEN Nishina Center (RNC), Saitama 351-0198, Japan*

[c]*RIKEN Center for Computational Science, Kobe 650-0047, Japan*

[d]*Department of Physics, Osaka University, Toyonaka 560-0043, Japan*

[e]*KEK Theory Center, High Energy Accelerator Research Organization (KEK), Tsukuba 305-0801, Japan*

[f]*School of High Energy Accelerator Science, The Graduate University for Advanced Studies (Sokendai), Tsukuba 305-0801, Japan*

[g]*Kobayashi-Maskawa Institute for the Origin of Particles and the Universe, Nagoya University, Nagoya 464-8602, Japan*

[h]*Advanced Science Research Center, Japan Atomic Energy Agency (JAEA), Tokai 319-1195, Japan*

E-mail: k.suzuki.2010@th.phys.titech.ac.jp

We study the $U(1)_A$ anomaly at high temperatures of $N_f = 2+1$ lattice QCD with chiral fermions. Gauge ensembles are generated with Möbius domain-wall (MDW) fermions, and the measurements are reweighted to those with overlap fermions. We report on the results for the Dirac spectra, the $U(1)_A$ susceptibility, and the topological susceptibility in the temperature range of $T = 136$, 153, 175, and 204 MeV, where the up and down quark masses are set to be near the physical point as well as at lighter or heavier masses.

The 40th International Symposium on Lattice Field Theory, LATTICE2023
July 31st - August 4th, 2023
Fermi National Accelerator Laboratory

1. Introduction

In quantum chromodynamics (QCD) describing dynamics of the quarks and gluons, key features are the $SU(2)_L \times SU(2)_R$ chiral symmetry (for up and down quarks near the massless limit) and the $U(1)_A$ symmetry. In the low-temperature phase of QCD, the chiral symmetry is spontaneously broken due to the chiral condensate, while the $U(1)_A$ symmetry is explicitly broken by the quantum anomaly. In the high-temperature phase, the chiral condensate is suppressed and the chiral symmetry is restored (for massless quarks), while the temperature-dependence of the $U(1)_A$ anomaly is not undestood well (for recent progress in lattice QCD simulations, see Ref. [1–4]).

The JLQCD collaboration has been working on this issue [5–8] by using lattice QCD simulations with chiral fermions, i.e., the overlap (OV) fermion formulation [9, 10]. Since the OV fermion formulation keeps tha chiral symmetry on the lattice and should be appropriate to examine physics related to the chiral and $U(1)_A$ symmetries. However, simulations with OV fermions require an enormous computational cost, so that we have to apply a technique to reduce the cost. For example, in Ref. [5] the topological sector was fixed to the trivial one. In Ref. [6–8], the MDW/OV reweighting technique [6, 11] was applied, where physical quantities measured on gauge ensembles generated with Möbius domain-wall (MDW) fermions [12–14] are reweighted to corresponding ones on OV fermion ensembles. So far, our simulations were mainly done with two flavors of quarks.

In this work, we study $N_f = 2 + 1$ QCD including the strange quark. In this contribution, we report on the preliminary results from $N_f = 2 + 1$ lattice QCD simulations. Some of results in high-temperature phase ($T = 204$ MeV and 175 MeV) were already reported in our previous proceedings [15], and here main updates are the results at lower temperatures: $T = 153$ MeV near the pseudocritical temperature and 136 MeV in the chiral symmtry broken phase.[1] Parameters of numerical lattice simulations are summarized in Table 1. We applied the tree-level Symanzik improved gauge action [16] and dynamical MDW fermion action [12–14], and measured quantities are reweighted to those with overlap fermions. The gauge coupling is set to be $\beta = 4.17$ which corresponds to the lattice cutoff $a^{-1} = 2.453$ GeV (or the lattice spacing $a \sim 0.08$ fm) determined in our simulations at zero temperature [17]. We generated gauge ensembles with the up and down quark masses in the range of $am_{ud} = 0.002$-0.0120, where $am_{ud} = 0.002$ ($m_{ud} \sim 4.9$ MeV) is considered to be near the physical point (if $m_{ud}^{\text{phys}} \sim 3.5$ MeV). In addition, the observables at $am_{ud} = 0.001$ ($m_{ud} \sim 2.5$ MeV lighter than the physical point) are obtained by the mass reweighting technique from the ensembles at $am_{ud} = 0.002$. The strange-quark mass is fixed to be $am_s = 0.04$ ($m_s \sim 98.1$ MeV near the physical point).

2. Overlap Dirac spectrum

First, we investigate the eigenvalue spectrum of the overlap Dirac operator,

$$\rho(\lambda) = \frac{1}{V} \sum_{\lambda_i} \langle \delta(\lambda - \lambda_i) \rangle, \tag{1}$$

where V is the volume, and λ_i is the i-th positive eigenvalue of the overlap Dirac operator. $\langle O \rangle$ means the gauge ensemble average of a quantity O. As is well known, the Banks-Casher relation [18],

---

[1]If the pseudocritical temperature is assumed to be $T_c = 155$ MeV, the four temperatures $T = 204, 175, 153,$ and 136 MeV are approximately $T \sim 1.3T_c, 1.1T_c, 1.0T_c,$ and $0.9T_c$, respectively.

Table 1: Numerical parameters of lattice simulations. $L^3 \times L_t$ are lattice size in the spatial and temporal directions. m_{ud} and m_s are the degenerate mass of up and down quarks and strange-quark mass, respectively.

$L^3 \times L_t$	T (MeV)	am_{ud}	m_{ud} (MeV)	am_s	Comments
$32^3 \times 12$	204	0.0010	2.5	0.040	m_{ud} by mass reweighting
$32^3 \times 12$	204	0.0020	4.9	0.040	
$32^3 \times 12$	204	0.0035	8.6	0.040	
$32^3 \times 12$	204	0.0070	17	0.040	
$32^3 \times 12$	204	0.0120	29	0.040	
$32^3 \times 14$	175	0.0010	2.5	0.040	m_{ud} by mass reweighting
$32^3 \times 14$	175	0.0020	4.9	0.040	
$32^3 \times 14$	175	0.0035	8.6	0.040	
$32^3 \times 14$	175	0.0050	12	0.040	
$32^3 \times 14$	175	0.0070	17	0.040	
$32^3 \times 14$	175	0.0120	29	0.040	
$32^3 \times 16, 40^3 \times 16$	153	0.0010	2.5	0.040	m_{ud} by mass reweighting
$32^3 \times 16, 40^3 \times 16$	153	0.0020	4.9	0.040	
$32^3 \times 16, 40^3 \times 16$	153	0.0035	8.6	0.040	
$32^3 \times 16, 40^3 \times 16$	153	0.0070	17	0.040	
$32^3 \times 16, 40^3 \times 16$	153	0.0120	29	0.040	
$36^3 \times 18, 48^3 \times 18$	136	0.0010	2.5	0.040	m_{ud} by mass reweighting
$36^3 \times 18, 48^3 \times 18$	136	0.0020	4.9	0.040	
$36^3 \times 18, 48^3 \times 18$	136	0.0035	8.6	0.040	
$36^3 \times 18, 48^3 \times 18$	136	0.0070	17	0.040	
$36^3 \times 18, 48^3 \times 18$	136	0.0120	29	0.040	

$\langle \bar{q}q \rangle = -\lim_{V \to \infty} \pi \rho(0)$, states that the chiral condensate $\langle \bar{q}q \rangle$ is proportional to the value of Dirac spectrum at $\lambda = 0$.

In Fig. 1, we show the Dirac spectra at $T = 153$ MeV (top panels) and 136 MeV (bottom panels). $T = 153$ MeV is near (or slightly lower than) the pseudocritical temperature in $N_f = 2 + 1$ QCD with the physical quark mass. While $\rho(0)$ is nonzero for heavier quark mass ($m_{ud} \gtrsim 4.9$ MeV), it is consistent with zero at the lightest quark mass ($m_{ud} \sim 2.5$ MeV), which suggests $\rho(0) \sim 0$ in the chiral limit ($m_{ud} \to 0$). On the other hand, since $T = 136$ MeV is below the pseudocritical temperature, $\rho(0)$ is nonzero at all the quark masses. Note that the horizontal line is the chiral condensate at zero temperature (divided by π), which was obtained in our previous simulations [19]. For Dirac spectra at higher temperatures ($T = 204$ and 175 MeV), see our previous proceedings [15].

In Fig. 2, we show the value of the the lowest bin of the Dirac spectrum as a function of m_{ud}. We confirm that, at the lightest quark mass, the lowest bin is strongly suppressed at $T = 153$-204 MeV, which is suggests that it is almost zero even in the chiral limit. On the other hand, at $T = 136$ MeV, the value of the lowest bin is nonzero, which is due to the chiral condensate.

3. $U(1)_A$ **susceptibility**

The $U(1)_A$ susceptibility is defined as the difference between the two-point mesonic correlators of the isovector-pseudoscalar channel π^a and isovector-scalar channel δ^a (the subscript a is the
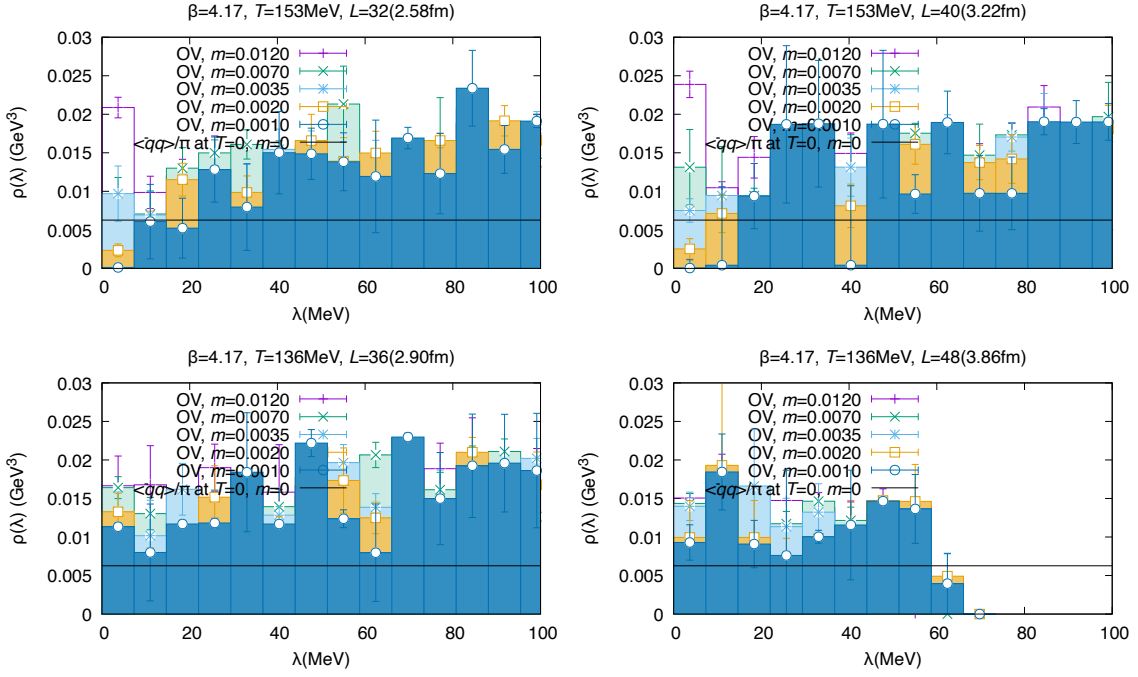
Figure 1: Dirac spectrum $\rho(\lambda)$ on reweighted OV ensembles at $T = 153$ (upper) and 136 MeV (lower). Results with two volumes are shown in left and right panels.
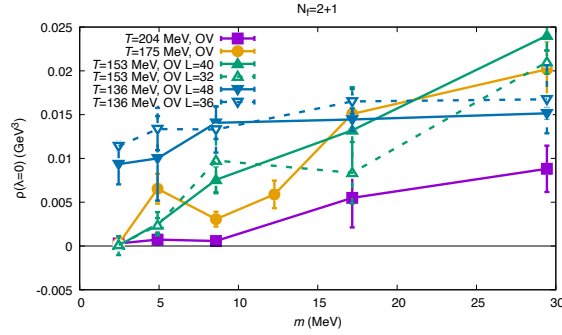

Figure 2: Quark mass dependence of lowest-bin value of Dirac spectrum, $\rho(\lambda = 0)$, at $T = 136$-204 MeV.

isospin index):

$$\Delta_{\pi-\delta} \equiv \chi_\pi - \chi_\delta \equiv \int d^4x \langle \pi^a(x)\pi^a(0) - \delta^a(x)\delta^a(0) \rangle. \tag{2}$$

On the lattice, $\Delta_{\pi-\delta}$ is calculated by the spectral decomposition of the overlap Dirac operator [20],

$$\Delta_{\pi-\delta}^{\text{ov}} = \frac{1}{V(1-m^2)^2} \left\langle \sum_i \frac{2m^2(1-\lambda_i^{(\text{ov},m)2})^2}{\lambda_i^{(\text{ov},m)4}} \right\rangle, \tag{3}$$
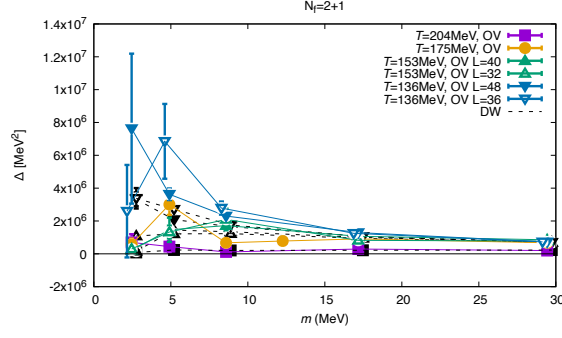
Figure 3: Quark mass dependence of $U(1)_A$ susceptibility $\Delta^{\text{ov}}_{\pi-\delta}$ at T = 136-204 MeV.

where $\lambda_i^{(\text{ov},m)}$ is the eigenvalue of the massive overlap Dirac operator $H_m = \gamma_5[(1-m)D_{\text{ov}} + m]$ with a mass m, and the lattice spacing is set as $a = 1$.[2]

In Fig. 3, we show the results for the $U(1)_A$ susceptibility. At T = 153-204 MeV, we find that the $U(1)_A$ susceptibility is strongly suppressed at the lightest quark mass, which suggests that the $U_1(A)$ susceptibility is consistent with zero in the chiral limit. On the other hand, in the chiral symmetry broken phase (T = 136 MeV), it is nonzero.

4. Topological susceptibility

The topological susceptibility is defined as

$$\chi_t \equiv \frac{\langle Q_t^2 \rangle}{V}, \tag{4}$$

with the gauge ensemble average of the topological charge Q_t for the gluon fields. In order to compute the topological charge, we apply two types of methods: (i) In the first method, the topological charge is obtained from the index of the overlap Dirac operator,

$$Q_t = n_+ - n_-, \tag{5}$$

where $n_\pm$ is the number of the zero modes with positive (+) or negative (-) chirality. (ii) In another method, the topological charge is defined by the field-strength tensor of gluon fields. In order to define it on the lattice, we apply the gradient flow [21] in the space of lattice gauge fields. Then,

$$Q_t(t) = \frac{1}{32\pi^2} \sum_x \varepsilon^{\mu\nu\rho\sigma} \text{Tr} \left[F_{\mu\nu}(x,t) F_{\rho\sigma}(x,t) \right], \tag{6}$$

where $F_{\mu\nu}(x,t)$ is a field-strength tensor of lattice gauge fields at spacetime x and a flow time t. In this work, we adopt the clover-type construction of $F_{\mu\nu}(x,t)$, and we pick the results at $ta^2 = 5$ (a plateau for $Q_t(t)$ is stable for $ta^2 \gtrsim 3$ [22]).

---

[2]Note that this is one of the simplest definitions with overlap Dirac eigenvalues. One can define other $U(1)_A$ susceptibilities by subtracting the contributions from chiral zero modes [6, 7] and/or from the logarithmic UV divergence [7]. In this work, we show results obtained without such subtraction schemes.
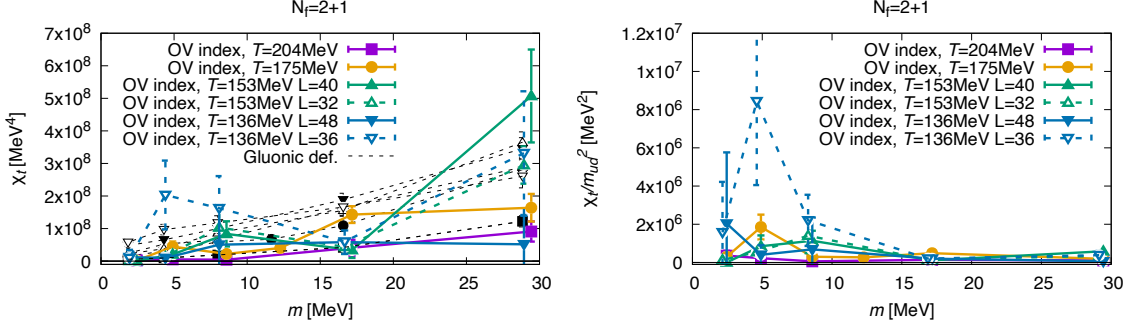
Figure 4: Quark mass dependence of topological susceptibilities χ_t and its divided quantities χ_t/m_{ud}^2 at $T = 136$-204 MeV. In the left panel, colored and black points represent χ_t from the fermionic definition (5) on reweighted OV ensembles and χ_t from the gluonic definition (6) on MDW ensembles, respectively.

In Fig. 4, we show the results for the quark mass dependence of the topological susceptibility. Since χ_t is expected to be proportional to m_{ud} in the chiral symmetry broken phase (e.g., at the leading order of the chiral perturbation theory [23]), we plot another quantity χ_t/m_{ud}^2 in order to check the scaling with m_{ud}. From the right panel, we find that χ_t/m_{ud}^2 at $T = 153$-204 MeV is strongly suppressed toward the chiral limit, whereas the result at $T = 136$ MeV stays at nonzero values. Thus, the behaviors of χ_t in the chiral symmetry broken phase and in the high-temperature phase are distinct.

5. Conclusion and outlook

In this contribution, we show the preliminary results for (i) Dirac spectra $\rho(\lambda)$, (ii) $U(1)_A$ susceptibilities $\Delta_{\pi-\delta}$, and (iii) topological suscptibilities χ_t in $N_f = 2 + 1$ lattice QCD simulations with chiral (i.e., reweighted overlap) fermions in the temperature range of $T = 136$-204 MeV. Dependences of these quantities on up and down quark masses are studied in the range of $m_{ud} = 2.5$-29 MeV, which covers not only the physical quark mass but also a lighter quark mass (i.e., near the chiral limit). Our results suggest that $\rho(0)$, $\Delta_{\pi-\delta}$, and χ_t/m_{ud}^2 in the chiral limit at $T = 153$-204 MeV (near and higher than the pseudocritical temperature) is strongly suppressed, while those at $T = 136$ MeV (in the low-temperature phase) are nonzero.

Finally, we give remarks on other measurements:

- *Chiral susceptibility*—The chiral susceptibility [24], defined as the first derivative of the chiral condensate with respect to the quark mass, is useful for estimating the pseudocritical temperature for the chiral condensation. Also, it can be related to the $U(1)_A$ and topological suscptibilities as well as the chiral condensate. Our previous results [8] at $N_f = 2$ suggest that both the connected and disconnected parts of the chiral susceptibility are dominated by the contribution from the $U(1)_A$ anomaly in the region of $m_{ud} \geq 2.64$ MeV at $T = 220$-330 MeV and also in $m_{ud} \geq 6.6$ MeV at $T = 190$ MeV (see Ref. [25] for $T = 165$ MeV). For our latest updates, see Ref. [26].

- *Hadronic correlators*—Also from mesonic/baryonic correlators, we can study the chiral and $U(1)_A$ symmetries from the viewpoint of a degeneracy between the correlators for their sym-

metry partners. In addition, in the high-temperature phase, not only the chiral and $U(1)_A$ symmetries but also an emergent symmetry can appear, which is called the chiral spin symmetry [27, 28] (see Ref. [29] for a recent review). The results [30, 31] for mesonic spatial correlators in $N_f = 2$ lattice QCD suggest that this symmetry is realized in the range of $T = 220\text{-}480$ MeV (see Ref. [32] for the temporal correlators). For our latest updates including $N_f = 2+1$ simulations, see Ref. [33].

Acknowledgment

References

[1] HotQCD collaboration, *Meson screening masses in (2+1)-flavor QCD*, *Phys. Rev.* **D100** (2019) 094510 [1908.09552].

[2] H.T. Ding, S.T. Li, S. Mukherjee, A. Tomiya, X.D. Wang and Y. Zhang, *Correlated Dirac Eigenvalues and Axial Anomaly in Chiral Symmetric QCD*, *Phys. Rev. Lett.* **126** (2021) 082001 [2010.14836].

[3] O. Kaczmarek, L. Mazur and S. Sharma, *Eigenvalue spectra of QCD and the fate of UA(1) breaking towards the chiral limit*, *Phys. Rev. D* **104** (2021) 094518 [2102.06136].

[4] O. Kaczmarek, R. Shanker and S. Sharma, *Eigenvalues of the QCD Dirac matrix with improved staggered quarks in the continuum limit*, *Phys. Rev. D* **108** (2023) 094501 [2301.11610].

[5] G. Cossu, S. Aoki, H. Fukaya, S. Hashimoto, T. Kaneko, H. Matsufuru et al., *Finite temperature study of the axial U(1) symmetry on the lattice with overlap fermion formulation*, *Phys. Rev. D* **87** (2013) 114514 [1304.6145].

[6] JLQCD collaboration, *Evidence of effective axial U(1) symmetry restoration at high temperature QCD*, *Phys. Rev. D* **96** (2017) 034509 [1612.01908].

[7] JLQCD collaboration, *Study of the axial U(1) anomaly at high temperature with lattice chiral fermions*, *Phys. Rev. D* **103** (2021) 074506 [2011.01499].

[8] JLQCD collaboration, *Role of the axial U(1) anomaly in the chiral susceptibility of QCD at high temperature*, *PTEP* **2022** (2022) 023B05 [2103.05954].

[9] H. Neuberger, *Exactly massless quarks on the lattice*, *Phys. Lett. B* **417** (1998) 141 [hep-lat/9707022].

[10] H. Neuberger, *A Practical implementation of the overlap Dirac operator*, *Phys. Rev. Lett.* **81** (1998) 4060 [hep-lat/9806025].

[11] JLQCD collaboration, *Overlap/Domain-wall reweighting*, *PoS* **LATTICE2013** (2014) 127 [1311.4646].

[12] R.C. Brower, H. Neff and K. Orginos, *Möbius fermions: Improved domain wall chiral fermions*, *Nucl. Phys. B Proc. Suppl.* **140** (2005) 686 [hep-lat/0409118].

[13] R.C. Brower, H. Neff and K. Orginos, *Möbius fermions*, *Nucl. Phys. Proc. Suppl.* **153** (2006) 191 [hep-lat/0511031].

[14] R.C. Brower, H. Neff and K. Orginos, *The Möbius domain wall fermion algorithm*, *Comput. Phys. Commun.* **220** (2017) 1 [1206.5214].

[15] JLQCD collaboration, *Axial U(1) symmetry at high temperatures in $N_f = 2 + 1$ lattice QCD with chiral fermions*, *PoS* **LATTICE2021** (2022) 332 [2203.16059].

[16] M. Lüscher and P. Weisz, *Computation of the Action for On-Shell Improved Lattice Gauge Theories at Weak Coupling*, *Phys. Lett. B* **158** (1985) 250.

[17] JLQCD collaboration, *Form factors of $B{\to}\pi\ell\nu$ and a determination of |Vub| with Möbius domain-wall fermions*, *Phys. Rev. D* **106** (2022) 054502 [2203.04938].

[18] T. Banks and A. Casher, *Chiral Symmetry Breaking in Confining Theories*, *Nucl. Phys. B* **169** (1980) 103.

[19] G. Cossu, H. Fukaya, S. Hashimoto, T. Kaneko and J.-I. Noaki, *Stochastic calculation of the Dirac spectrum on the lattice and a determination of chiral condensate in 2+1-flavor QCD*, *PTEP* **2016** (2016) 093B06 [1607.01099].

[20] JLQCD collaboration, *Violation of chirality of the Möbius domain-wall Dirac operator from the eigenmodes*, *Phys. Rev. D* **93** (2016) 034507 [1510.07395].

[21] M. Lüscher, *Properties and uses of the Wilson flow in lattice QCD*, *JHEP* **08** (2010) 071 [1006.4518].

[22] ALPHA collaboration, *Topological susceptibility and the sampling of field space in $N_f = 2$ lattice QCD simulations*, *JHEP* **08** (2014) 150 [1406.5363].

[23] H. Leutwyler and A.V. Smilga, *Spectrum of Dirac operator and role of winding number in QCD*, *Phys. Rev. D* **46** (1992) 5607.

[24] F. Karsch and E. Laermann, *Susceptibilities, the specific heat and a cumulant in two flavor QCD*, *Phys. Rev. D* **50** (1994) 6954 [hep-lat/9406008].

[25] JLQCD collaboration, *What is chiral susceptibility probing?*, *PoS* **LATTICE2021** (2022) 050 [2111.02048].

[26] JLQCD collaboration, *Chiral susceptibility and axial U(1) anomaly near the (pseudo-)critical temperature*, Contribution to LATTICE2023 .

[27] L. Ya. Glozman, *SU(4) symmetry of the dynamical QCD string and genesis of hadron spectra*, *Eur. Phys. J. A* **51** (2015) 27 [1407.2798].

[28] L. Ya. Glozman and M. Pak, *Exploring a new SU(4) symmetry of meson interpolators*, *Phys. Rev. D* **92** (2015) 016001 [1504.02323].

[29] L. Ya. Glozman, *Chiral spin symmetry and hot/dense QCD*, *Prog. Part. Nucl. Phys.* **131** (2023) 104049 [2209.10235].

[30] C. Rohrhofer, Y. Aoki, G. Cossu, H. Fukaya, L. Ya. Glozman, S. Hashimoto et al., *Approximate degeneracy of J = 1 spatial correlators in high temperature QCD*, *Phys. Rev. D* **96** (2017) 094501 [1707.01881].

[31] C. Rohrhofer, Y. Aoki, G. Cossu, H. Fukaya, C. Gattringer, L. Ya. Glozman et al., *Symmetries of spatial meson correlators in high temperature QCD*, *Phys. Rev. D* **100** (2019) 014502 [1902.03191].

[32] C. Rohrhofer, Y. Aoki, L. Ya. Glozman and S. Hashimoto, *Chiral-spin symmetry of the meson spectral function above T_c*, *Phys. Lett. B* **802** (2020) 135245 [1909.00927].

[33] JLQCD collaboration, *Study of Chiral Symmetry and $U(1)_A$ using Spatial Correlators for $N_f = 2 + 1$ QCD at finite temperature with Domain Wall Fermions*, Contribution to LATTICE2023 .

[34] G. Cossu, J. Noaki, S. Hashimoto, T. Kaneko, H. Fukaya, P.A. Boyle et al., *JLQCD IroIro++ lattice code on BG/Q*, *PoS* **LATTICE 2013** (2013) 482 [1311.0084].

[35] P. Boyle, A. Yamaguchi, G. Cossu and A. Portelli, *Grid: A next generation data parallel C++ QCD library*, *PoS* **LATTICE 2015** (2015) 023 [1512.03487].

[36] N. Meyer, P. Georg, S. Solbrig and T. Wettig, *Grid on QPACE 4*, *PoS* **LATTICE2021** (2022) 068 [2112.01852].

[37] S. Ueda, S. Aoki, T. Aoyama, K. Kanaya, H. Matsufuru, S. Motoki et al., *Development of an object oriented lattice QCD code "Bridge++"*, *J. Phys. Conf. Ser.* **523** (2014) 012046.

[38] Y. Akahoshi, S. Aoki, T. Aoyama, I. Kanamori, K. Kanaya, H. Matsufuru et al., *General purpose lattice QCD code set Bridge++ 2.0 for high performance computing*, *J. Phys. Conf. Ser.* **2207** (2022) 012053 [2111.04457].